Charge ordered state and giant magnetoresistance in $Pr_{0.7}R_{0.1}Ca_{0.2}MnO_3$ (R = Y, Dy, Gd, Sm, Nd)

1998 J. Phys.: Condens. Matter 10 L199

(http://iopscience.iop.org/0953-8984/10/13/001)

J. Phys.: Condens. Matter **10** (1998) L199–L205. Printed in the UK PII: S0953-8984(98)91404-7

LETTER TO THE EDITOR

Charge ordered state and giant magnetoresistance in $Pr_{0.7}R_{0.1}Ca_{0.2}MnO_3$ (R = Y, Dy, Gd, Sm, Nd)

A Barman, M Ghosh, S Biswas, S K De and S Chatterjee

Department of Materials Science, Indian Association for the Cultivation of Science, Jadavpur, Calcutta 700 032, India

Received 6 February 1998

Abstract. The partial substitution of Pr by the rare earth elements (Y, Dy, Gd, Sm, Nd) in $Pr_{0.8}Ca_{0.2}MnO_3$ induces charge ordering at 120 K. The insulator to metal transition associated with a large negative magnetoresistance has been observed in the presence of magnetic field. The metallic state is destroyed under application of magnetic field and returns to an insulating state at low temperature. The magnetoresistance reveals a broad maximum upon cooling from 150 to 100 K. These results are interpreted by double-exchange interaction and Jahn–Teller distortion.

The transport properties of manganese perovskites $R_{1-x}A_xMnO_3$, where R is the rare earth element and A is the divalent alkaline earth ions, have attracted much attention due to the recent discovery of giant magnetoresistance (GMR) [1–3]. The large negative magnetoresistance has been observed at the insulator–metal transition with the simultaneous appearance of paramagnetic–ferromagnetic transition for the doping level $0.3 \leqslant x < 0.5$. Such a behaviour is generally explained in terms of double-exchange interaction [4–6] and Jahn–Teller distortion [7]. For the composition around $x = 0.5$, a real space ordering of Mn^{3+} and Mn^{4+} ions occurs known as charge ordering (CO), in many perovskite oxides such as $La_{0.5}Ca_{0.5}MnO_3$ [8], $Pr_{0.5}Sr_{0.5}MnO_3$ [3, 9] and $Nd_{0.5}Sr_{0.5}MnO_3$ [10]. The CO transition is followed by the ferromagnetic (FM) metal to antiferromagnetic (AFM) insulator transition as the temperature is lowered.

The manganite $Pr_{1-x}Ca_xMnO_3$, with relatively small one-electron band width, is interesting due to the appearance of the CO state for a wider range of $x(0.3 \leqslant x \leqslant 0.75)$ around 0.5 [11–13]. The substitution of various metallic ions for manganese modifies dramatically the transport and magnetic properties of this system [14]. The stability of the CO state in $Pr_{1-x}Ca_xMnO_3$ against the chemical pressure produced by the partial replacement of Ca with Sr has been studied in detail [15–18]. Application of magnetic field can melt the CO state and lead to the insulator to metal transition accompanied by a large drop in resistivity of the material [17, 18]. Most of the previous works on the transport properties are concentrated on the composition range $0.3 \leqslant x < 0.5$. However, the transport properties have not yet been studied in detail for $x < 0.3$ and also the mechanism for the CO state has not been developed so far. The electronic and magnetic properties of the manganite perovskites are strongly dependent on the nature and the ionic radii of the interpolated cations (Pr, R). In this letter, we present the electrical properties of $Pr_{1-x}Ca_xMnO_3$ for the low doping level $x = 0.2$ by replacing Pr with rare earth elements having smaller ionic radii such as Y, Dy, Gd, Sm and Nd at low temperature and in high magnetic field.

0953-8984/98/130199+07$19.50

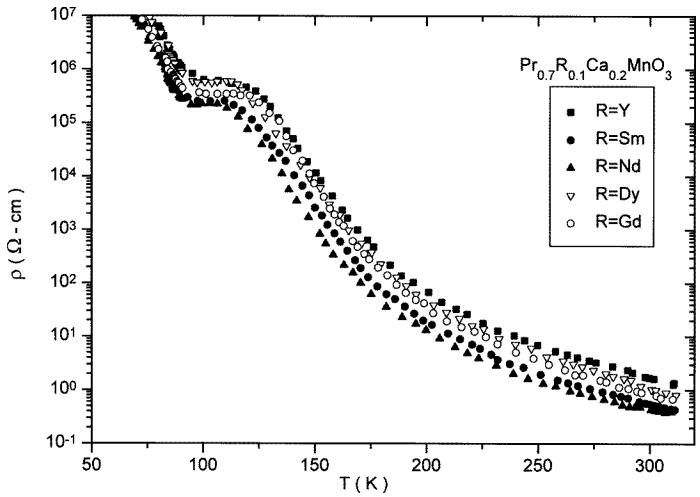

Figure 1. Resistivity ($\rho(\Omega$ cm)) is plotted against temperature (K) at zero magnetic field. The symbols are indexed at the top right corner of the figure.

The five samples with nominal composition $Pr_{0.7}R_{0.1}Ca_{0.2}MnO_3$ (R = Y, Dy, Gd, Sm, Nd) have been prepared by the standard ceramic technique. Appropriate amounts of Pr_6O_{11}, $CaCO_3$, $MnCO_3$ and $Y_2O_3/Dy_2O_3/Gd_2(CO_3)_3/Sm_2(CO_3)_3/Nd_2(CO_3)_3$ are taken respectively, maintaining the stoichiometric ratio, and mixed with distilled ethanol for quite a long time to obtain a homogeneous mixture. The mixtures were then dried and the powders were calcined in open air at 900 °C for 24 hours. The calcined powders were then ground, pressed into pellets with a pressure of three tons and sintered in open air at 1200 °C for 24 hours. For obtaining better crystallization this process was repeated three times. Finally the samples were sintered at 1300 °C for 24 hours. X-ray diffraction patterns with Cu Kα radiation have confirmed the single-phase perovskite structure of all the samples with no significant trace of impurity.

Rectangular pieces of the samples with approximate dimensions 10 mm × 2 mm × 1 mm were cut for the resistivity measurement. Four leads were connected on the samples by means of ultrasonic soldering. The linear current–voltage characteristics at several fixed temperatures confirmed the ohmic electrical contacts of the leads. The resistivities of the samples were measured using a standard four-probe method within a temperature range of 4.2–300 K and magnetic field range 0–7.5 Tesla in a ^{4}He cryostat, equipped with a superconducting magnet. However for almost all the samples the magnitude of resistivity below 60 K has become very large and goes beyond our measurement facility.

The temperature dependences of the resistivity, $\rho(T)$ for $Pr_{0.7}R_{0.1}Ca_{0.2}MnO_3$ samples in the absence of magnetic field are shown in figure 1. The room-temperature resistivity increases as the ionic radius of R decreases from 1.163 Å (Nd) to 1.075 Å (Y). The resistivity increases with the lowering of temperature for all the samples. An abrupt change in the resistivity has been observed around 120 K. Such an anomaly in resistivity is due to the onset of the CO state. The manganite $Pr_{1-x}Ca_xMnO_3$ remains an insulator for all values of x due to the smaller ionic radii of Pr^{3+} and Ca^{2+} cations. Recently, it has been found that the CO state appears at 250 K only for $x \geqslant 0.3$ [13]. Figure 1 indicates that the substitution of Pr by another rare earth induces the CO state at much lower temperature, about 120 K for $x = 0.2$. The interesting fact is that the charge ordering transition temperature T_{CO} does

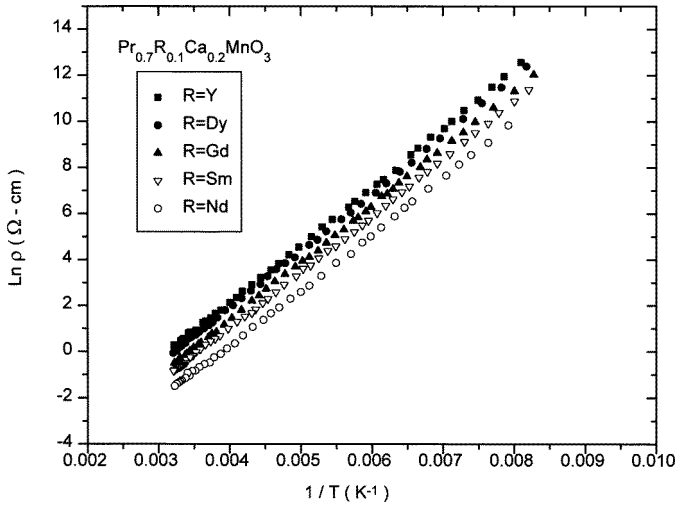

(a)

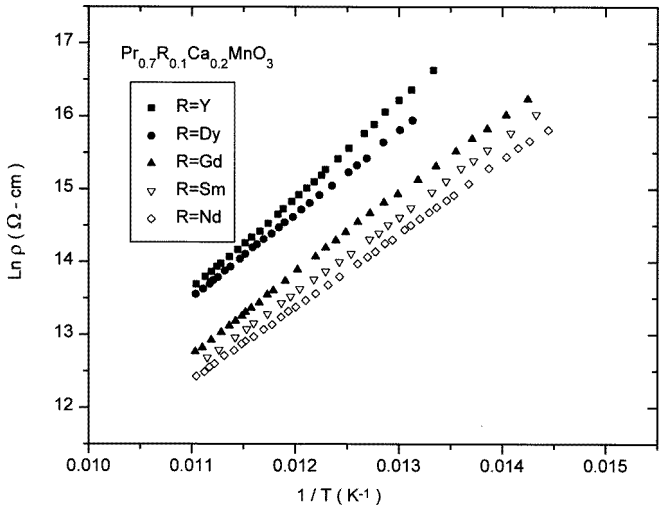

(b)

Figure 2. (a) $\ln \rho(\Omega\ \mathrm{cm})$ is plotted against $1/T$ (K^{-1}) in the temperature interval of 120–300 K. The symbols are indexed in the top left corner of the figure. (b) $\ln \rho(\Omega\ \mathrm{cm})$ is plotted against $1/T$ (K^{-1}) in the temperature region below 90 K. The symbols are indexed at the top left corner of the figure.

not change significantly with the substituted rare earth ions.

Figures 2(a) and 2(b) show the $\ln \rho$–T^{-1} plot for all the samples in two different temperature regions, the first one for the higher-temperature region 120–300 K and another one for the lower-temperature region below 90 K. The intermediate temperature shows sudden discontinuity in the semiconducting behaviour and shows a slight increase in resistivity with temperature. All the samples show very good linear behaviour in the $\ln \rho$–T^{-1} plot for both the temperature regions. Hence the conduction occurs through a thermally activated process. However the slopes for the different temperature regions for any of the samples are different. The activation energies obtained from the slopes of the linear curves

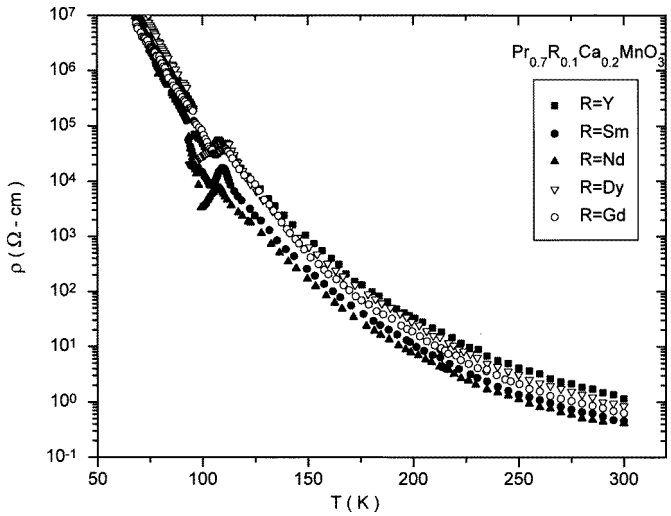

Figure 3. Resistivity ($\rho(\Omega$ cm)) is plotted against temperature (K) at magnetic field, $H =$ 7.5 Tesla. The symbols are indexed at the top right corner of the figure.

of $\ln\rho$–$1/T$ plots are 86 meV for Nd, 91 meV for Sm, 94 meV for Gd, 99 meV for Dy and 112 meV for the Y substituted sample in the temperature region below 90 K. For the higher-temperature region, above 120 K, the activation energies are 207 meV, 210 meV, 214 meV, 215 meV and 217 meV for substitution with Nd, Sm, Gd, Dy and Y respectively. The activation energies both at high and low temperatures increases slightly with the decrease of ionic radius of R.

The variation of resistivity as a function of temperature in the presence of magnetic field 7.5 T is depicted in figure 3 for all the samples. The resistivity increases with the decrease of temperature from 300 K to about 100 K for all of the samples. The magnitude of the resistivity is lower than the zero-field value throughout the whole temperature interval. The insulator to metal transition has been observed around 100 K which is not observed in the parent material $Pr_{0.8}Ca_{0.2}MnO_3$ up to a magnetic field of 8 T [13]. The metallic phase persists for a small temperature interval and all the samples return to an insulating state around 90 K. The change in the slope in ρ–T curves below 90 K suggests that the CO state is not collapsed at a magnetic field of 7.5 T. The noticeable fact is that the insulator to metal transition (T_{IM}) temperature is very close to the charge ordering temperature (T_{CO}). These facts are quite different from the undoped manganites $Pr_{1-x}Ca_xMnO_3$ with $x \geqslant 0.3$ in which the CO state has completely disappeared at 8 T and T_{IM} is much lower than T_{CO} [13, 15, 16].

The field induced insulator to metal transition is associated with a transition to ferromagnetic state. However in this small metallic region, the resistivity shows a very good linear nature when plotted against T^2 as shown in figure 4. This suggests that the temperature dependence of the resistivity in this metallic region can be described by the relation $\rho(T) = \rho(0) + AT^2$ and the electron–electron scattering process associated with spin fluctuation plays an important role in the present manganites. The values of the coefficient A obtained from the slope of the ρ–T^2 plot are 3.12 Ω cm K^{-2}, 7.23 Ω cm K^{-2}, 8.37 Ω cm K^{-2}, 8.98 Ω cm K^{-2} and 24 Ω cm K^{-2} for substitution with Nd, Sm, Gd, Dy and Y respectively. The values of A are very large compared to that of a normal metal and it may be due to the very large magnitude of the resistivity itself of these materials in this

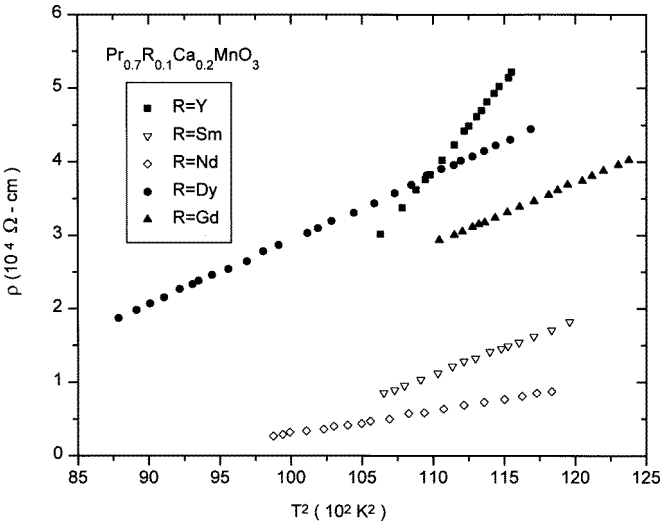

Figure 4. Resistivity ($\rho(10^4\ \Omega\ \mathrm{cm})$) is plotted against T^2 ($10^2\ \mathrm{K}^2$). The symbols are indexed at the top left corner of the figure.

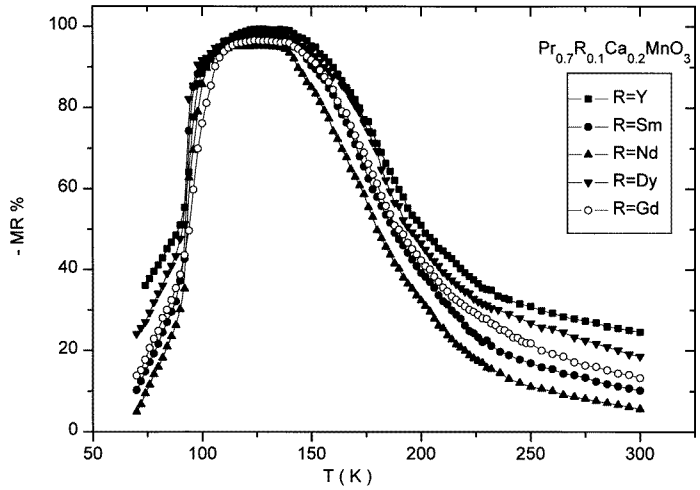

Figure 5. Negative magnetoresistance percentage ($-$MR%) is plotted against temperature (K). The symbols are indexed at the top right corner of the figure.

temperature region. The coefficient A increases with the decrease of the ionic radius of R.

Figure 5 shows the plot of negative magnetoresistance percentage ($-$MR%), defined as $(\rho(H,\ T)-\rho(0,\ t))/\rho(0,\ T)\times 100\%$, as a function of temperature, at a fixed magnetic field of 7.5 T. The $-$MR% increases with decrease of temperature down to 150 K and remains almost constant down to 100 K and then decreases sharply. The $-$MR% reveals a broad maximum in the temperature interval between 150 and 100 K. The value of $-$MR% at the higher- and lower-temperature region increases systematically from Nd to Y substitution as the ionic radius decreases. However in the intermediate-temperature region where the broad maximum occurs the differences between the magnitude of $-$MR% are small although the

same trend is almost maintained. A maximum $-$MR% of 99.36% is obtained for the Y substituted sample whereas for the Nd substituted sample the maximum $-$MR% obtained is 95.4%.

In general, the charge ordering phenomenon occurs in a material with a relatively narrow electron band width. For the perovskite oxides, $R_{1-x}A_xMnO_3$, the band width strongly depends on the ionic radii of (R, A) ions or the tolerance factor. The replacement of R by the smaller ionic radius will cause a tilting of MnO_6 octahedra and a decrease of Mn–O–Mn bond angle. These lead to distortion dependent reduction in one electron band width through the tolerance factor. The DE arises from the itinerancy of charge carriers. Thus the reduction in band width weakens the DE interaction. The CO state is most stable for the composition $x = 0.5$. The appearance of the CO state for $x = 0.2$ indicates that the Jahn–Teller distortion and the antiferromagnetic superexchange interaction (Mn^{3+}–O–Mn^{3+}) play important roles due to the high concentration of Mn^{3+} ions. The Jahn–Teller distortion of Mn^{3+} lowers the energy of the e_g state and AFM superexchange gives rise to antiparallel spin alignments. These effects prevent hopping of electrons through the Mn–O–Mn path and favour charge localization, which finally gives rise to charge ordering at low temperature.

The field induced insulator to metal transition associated with the magnetic transition from a canted antiferromagnetic to ferromagnetic state can be described qualitatively by the DE mechanism. According to this mechanism, the charge transfer interaction between Mn^{3+} and Mn^{4+} ions can be expressed as $t = t_0 \cos(\theta)$, where θ is the relative angle of the local t_{2g} spins and t_0 is the transfer interaction in the fully spin polarized state. In zero field, the canted AFM state, $\theta \neq 0$, is insulating due to the decreased transfer interaction. Application of magnetic field leads to the FM state, $\theta = 0$, and consequently the transfer interaction is increased. This will enhance the DE interaction and the system is driven into a metallic state. In the metallic phase, the resistivity is very high (10^3 Ω cm) in contrast to the other manganites $Pr_{1-x}Ca_xMnO_3$ with $x \geqslant 0.3$ (10^{-3} Ω cm). The tolerance factor (0.88) of the present manganites is smaller than the most stable charge ordered material $Pr_{0.5}Ca_{0.5}MnO_3$ (0.89). The remarkable fact is that the present manganites exhibit a field induced insulator–metal transition while the material $Pr_{0.5}Ca_{0.5}MnO_3$ remains an insulator up to 8 T [13].

In summary, the effect of the substitution of Pr by the other rare earth elements on the electrical properties of $Pr_{0.8}Ca_{0.2}MnO_3$ at low temperature has been investigated. In zero field, the samples remain insulators down to 4.2 K and exhibit charge ordering at about 120 K. The magnetic field induces an insulator to metal transition accompanied by a large drop in resistivity corresponding to a $-$MR% of about 99.36%. The anomalous transport properties of $Pr_{0.7}R_{0.1}Ca_{0.2}MnO_3$ (R = Y, Dy, Gd, Sm, Nd) in comparison with other manganites illustrate that a strong correlation exists among the lattice distortion due to the lattice mismatch, antiferromagnetic superexchange interaction and Jahn–Teller distortion.

The experiment was performed under the financial support of the Department of Science and Technology, Government of India. One of the authors (M Ghosh) gratefully acknowledges UGC for a senior research fellowship.

References

[1] von Helmolt R, Wecker J, Holzapfel B, Schultz L and Samwer K 1993 *Phys. Rev. Lett.* **71** 2331
[2] Jin S, Tiefel T H, McCormack M, Fastnacht R A, Ramesh R and Chen L H 1994 *Science* **264** 413
[3] Tomioka Y, Asamitsu A, Moritomo Y, Kuwahara H and Tokura Y 1995 *Phys. Rev. Lett.* **74** 5108
[4] Zener C 1951 *Phys. Rev.* **82** 403
[5] Anderson P W and Hasegawa H 1955 *Phys. Rev.* **100** 675

[6] de Gennes P G 1960 *Phys. Rev.* **118** 141
[7] Millis A J, Littlewood P B and Shraiman B I 1995 *Phys. Rev. Lett.* **74** 5144
[8] Chen C H and Cheong S-W 1996 *Phys. Rev. Lett.* **76** 4042
[9] Knizek K, Jirak Z, Pollert E, Zounova F and Vratislav S 1992 *J. Solid State Chem.* **100** 292
[10] Kuwahara H, Tomioka Y, Asamitsu A, Moritomo Y and Tokura Y 1995 *Science* **270** 961
[11] Pollert E, Krupicka S and Kuzmicova E 1982 *J. Phys. Chem. Solids* **43** 1137
[12] Jirak Z, Krupicka S, Simsa Z, Dlouba M and Vratislav S 1985 *J. Magn. Magn. Mater.* **53** 153
[13] Lees M R, Barratt J, Balakrishnan G, Paul D McK and Dewhurst C D 1996 *J. Phys.: Condens. Matter* **8** 2967
[14] Raveau B, Maignan A and Martin C 1997 *J. Solid State Chem.* **130** 162
[15] Yoshizawa R, Kajimoto R, Kawano H, Tomioka Y and Tokura Y 1997 *Phys. Rev.* B **55** 2729
[16] Tomioka Y, Asamitsu A, Kuwahara H and Tokura Y 1997 *J. Phys. Soc. Japan* **66** 302
[17] Tomioka Y, Asamitsu A, Kuwahara H, Moritomo Y and Tokura Y 1996 *Phys. Rev.* B **53** R1689
[18] Yoshizawa H, Kawano H, Tomioka Y and Tokura Y 1996 *J. Phys. Soc. Japan* **65** 1043